

Oct 18th, 12:00 AM

Ultimate Behaviour of Trapezoidal Steel Sheets in Bending

Raffaele Landolfo

Fredrico M. Mazzolani

Follow this and additional works at: <https://scholarsmine.mst.edu/isccss>



Part of the [Structural Engineering Commons](#)

Recommended Citation

Landolfo, Raffaele and Mazzolani, Fredrico M., "Ultimate Behaviour of Trapezoidal Steel Sheets in Bending" (1994). *International Specialty Conference on Cold-Formed Steel Structures*. 3.
<https://scholarsmine.mst.edu/isccss/12iccfss/12iccfss-session4/3>

This Article - Conference proceedings is brought to you for free and open access by Scholars' Mine. It has been accepted for inclusion in International Specialty Conference on Cold-Formed Steel Structures by an authorized administrator of Scholars' Mine. This work is protected by U. S. Copyright Law. Unauthorized use including reproduction for redistribution requires the permission of the copyright holder. For more information, please contact scholarsmine@mst.edu.

ULTIMATE BEHAVIOUR OF TRAPEZOIDAL STEEL SHEETS IN BENDING

Raffaele Landolfo¹ - Federico M. Mazzolani²

ABSTRACT

A systematic analysis of existing trapezoidal steel sheets commonly used in the market is performed in order to compare their carrying capacity at the light of their ultimate behaviour. The complete investigation has been developed both from theoretical and experimental points of view. In this paper, the description of the experimental techniques, the numerical simulation of the obtained results as well as the exploitation of these data in order to check the codified design rules are reported.

1. INTRODUCTION

The structural behaviour of cold-formed steel sections is a research subject which has been carried out in the last decade in the range of activity of the Institute of Tecnica delle Costruzioni of the Engineering Faculty of the University of Naples. As far as sheetings are concerned, a great attention has been devoted to the innovative products, the so-called third generation of trapezoidal sheets such as TRP 200 [1,2].

In the field of traditional sheetings, the recent technical literature [3] called the attention on the importance to analyse the influence of the shape of the cross-section and of the presence of stiffeners in the compressed parts. On the other hand, it was observed that the shapes of the existing commercial sheetings are usually designed on the base of serviceability requirements on the base of empirical data and very seldom they have been examined from the point of view of their ultimate behaviour by means of refined research methodology.

With these motivations, a general research programme has been promoted on the bending behaviour of trapezoidal steel sheets commonly used in practice for roofing. The complete study has been carried out through the following phases:

- a) Experimental investigation on the behaviour under bending action of several trapezoidal steel sheets with different dimensions and thicknesses;
- b) Numerical evaluation of the bending process of the section taking into account the local instability phenomena of compressed parts by means of general simulation procedure;
- c) Evaluation of bending strength according to the main provisions and comparison with numerical and experimental results.

This programme has been developed with the cooperation of CREA (Massa) and CSM (Roma), the last being performed the experimental part [4]. The research is now concluded and a first elaboration of testing and simulation results has been done [5,6].

1 Research Assistant, University of Naples, Italy

2 Professor of Structural Engineering, University of Naples, Italy

2. EXPERIMENTAL ACTIVITY

2.1 Specimens selection

The experimental phase has been carried out by means of 32 bending tests on 16 different specimens. Nine shapes of trapezoidal sheets have been preliminary selected among the ones most widely used in practice for roofing (fig.1). Except for the first two shapes, which are symmetric about the horizontal axis, the other seven can generate two different specimens each other by overturning the cross section. Therefore, starting from the nine basic sheets, 16 different prototypes have been generated.

In order to interpret the obtained test results, these specimens have been subdivided in two group. According to the behavioural classes proposed in Eurocode 3, as classification parameter the b/t ratio of the compressed flanges has been assumed. Two groups are therefore obtained (fig.1): *1th group*, including specimens with $b/t < 41$ (n. 1, 4, 6, 8, 11, 13, 15);

2th group, including specimens with $b/t > 41$ (n. 2, 3, 5, 7, 9, 10, 12, 14, 16).

Each specimen is made of a single fold; the nominal dimensions of the cross-sections are shown in tab. 1. In such table, the actual dimensions measured in one section of each specimen are also reported. The geometrical properties of the cross-sections, evaluated according to the nominal and the actual dimensions, are given in tab. 2.

The comparison between nominal and actual geometry shows a significant disagreement, due to manufacturing tolerances. As far as the thickness is concerned, the maximum scatter ranges from -21% to +26%, varying from a minimum of 0.79 mm to a maximum of 1.26 mm. More complex is to comment the differences among each dimension of the cross-section, some of them being modified by the cutting process. A global judgement may be expressed by comparing the strength moduli of the nominal and the actual cross-section (tab. 2). This comparison shows that, sometimes, the scatter may reach the value of 30-35% (i.e. specimen 3B). Significant dimensional variations have been observed also between the two specimens (called A and B) of the same type of shape. In this case, the above mentioned scatter is usually close to 10% except for profiles n. 2, 3, 10, 12, and 16 having scatters of about 20-24%. From these results it appears that the manufacturing tolerances for sheetings are very rough and the use of the nominal values in the calculations can lead to unsafe results.

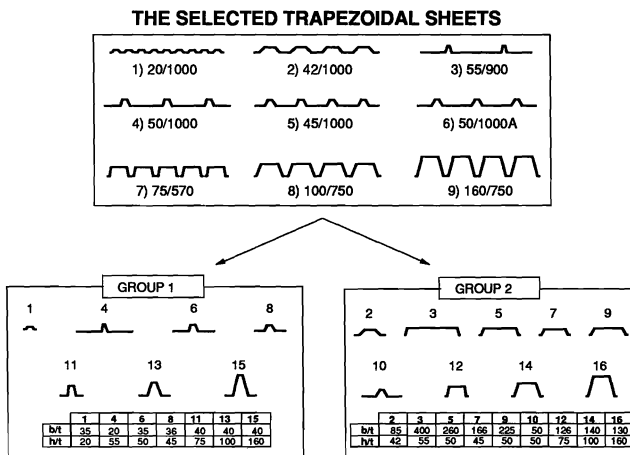
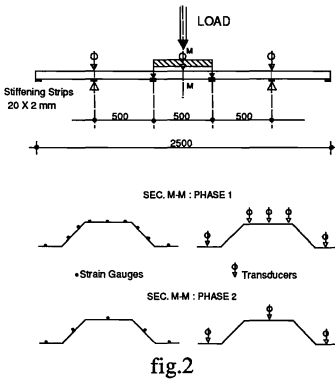


fig.1

2.2 Experimental tests

The experimental measurement system was designed in order to allow the evaluation of the specimen global response as well as the local behaviour of the midspan section where the strain gauges have been located. Monotonic tests have been performed on 32 simply supported beams with 1500 mm of span. Two concentrated loads have been applied in two sections spaced 500 mm across the midspan (fig. 2). The stiffening strips are located, each 50 mm, between the two bottom flanges, in order to guarantee the transversal cross-section indeformability, according to the actual boundary conditions. In a first phase, vertical displacements have been measured by means of transducers located in seven points (5 at midspan and 2 at supports). Bi-directional strain gauges in number of 9 to 12, have been distributed along the midspan cross-section. Furthermore, the number of transducers and strain gauges has been reduced to 3 and 5 respectively as shown in fig. 2. The ultimate values of testing loads are given in tab.3. More detailed informations concerning the test equipments and results are reported in [6].



The evaluation of the material mechanical properties has been done by means of 16 tension tests on strips obtained from each prototype. The results are shown in fig.3. All values evidence a significant variability. The statistical evaluation of these test results allows to determine the characteristic values of yield and ultimate strength which are $f_{y,k}=271 \text{ Nmm}^{-2}$ and $f_{t,k}=352 \text{ Nmm}^{-2}$, respectively. Such values are evaluated on the basis of 15 test results, excluding test n. 10 which provided a quite anomalous result, and assuming $k=2.57$ according to Italian provision for material qualification.

Furthermore, these characteristic values are comparable to the nominal values for Fe E 250 G steel grade ($f_{y,d}=250 \text{ Nmm}^{-2}$ and $f_{t,d}=330 \text{ Nmm}^{-2}$), which is commonly used for producing the examined sheets.

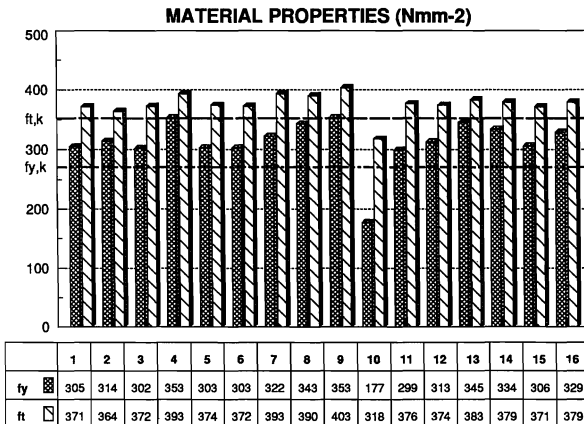



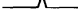




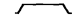






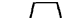








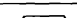

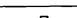


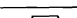

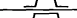


fig.3

DIMENSIONS (mm)		NOMINAL					ACTUAL					
n	SECTION	t	a	b	c	h	t	a	b	c	h	
1		1.0	100	35	65	20	A	1.01	126	33	62	20
							B	1.01	98	33	65	20
2		1.0	250	85	165	42	A	0.88	250	82	165	38
							B	1.02	250	82	165	43
3		1.0	450	400	430	55	A	1.01	458	379	421	50
							B	0.98	446	317	414	60
4		1.0	450	20	50	55	A	0.98	445	20	47	57
							B	0.97	445	21	50	57
5		1.0	333	260	298	50	A	1.01	326	260	285	50
							B	0.97	324	257	292	51
6		1.0	333	35	73	50	A	1.01	330	32	74	53
							B	0.98	325	32	67	52
7		1.0	250	166	214	45	A	1.05	247	160	215	48
							B	0.99	245	163	211	45
8		1.0	250	36	84	45	A	1.00	243	33	78	47
							B	1.02	245	33	81	47
9		1.0	333	223	283	50	A	1.01	336	224	282	50
							B	1.03	330	220	280	51
10		1.0	333	50	110	50	A	0.80	327	47	108	50
							B	1.01	326	47	108	50
11		1.0	190	40	64	75	A	0.96	187	36	63	76
							B	1.02	190	36	68	78
12		1.0	190	126	150	75	A	1.00	190	126	158	76
							B	1.26	190	122	154	75
13		1.0	250	40	110	100	A	0.96	249	36	110	102
							B	1.02	250	37	112	103
14		1.0	250	140	210	100	A	1.01	254	137	220	97
							B	0.79	250	137	210	101
15		1.0	250	40	120	160	A	0.98	250	36	115	163
							B	1.00	248	37	122	163
16		1.0	250	130	210	160	A	0.96	250	131	207	162
							B	1.26	250	128	210	162

Tab.1

PROPERTIES		NOMINAL				ACTUAL					
n	SECTION	A	I _x	W _x	P	A		I _x	W _x	ΔW _x	P
		cm ²	cm ⁴	cm ³	N/m	cm ²	cm ⁴	cm ³	2	N/m	
1		1.17	0.76	0.76	9.20	A	1.45	0.95	0.79	6	11.40
						B	1.16	0.74	0.74		
2		2.83	8.69	4.14	22.30	A	2.44	6.15	3.21	24	19.20
						B	2.90	9.21	4.24		
3		5.29	13.15	2.80	41.50	A	5.25	13.55	3.30	23	41.20
						B	4.90	20.14	4.30		
4		5.29	13.15	2.80	41.50	A	5.19	14.04	2.89	1	40.70
						B	5.12	14.17	2.93		
5		3.97	11.97	3.08	31.20	A	4.02	12.75	3.31	12	31.60
						B	3.80	11.63	2.92		
6		3.97	11.97	3.08	31.20	A	4.01	13.37	3.25	7	31.50
						B	3.87	12.32	3.03		
7		3.00	8.55	2.67	23.60	A	3.14	9.89	2.90	12	24.60
						B	2.92	8.22	2.56		
8		3.00	8.55	2.67	23.60	A	2.98	9.04	2.68	3	23.40
						B	3.04	9.24	2.75		
9		3.86	13.90	3.86	30.3	A	3.94	14.51	4.07	0	30.10
						B	3.96	14.87	4.07		
10		3.86	13.90	3.86	30.3	A	3.04	10.89	3.02	20	23.90
						B	3.82	13.57	3.76		
11		3.11	25.67	5.38	24.40	A	2.96	24.51	5.03	9	24.90
						B	3.17	27.53	5.55		
12		3.11	25.67	5.38	24.40	A	3.07	24.76	5.00	22	24.10
						B	3.83	30.59	6.38		
13		3.87	54.08	8.61	30.40	A	3.72	52.95	8.22	8	29.20
						B	3.97	57.76	8.92		
14		3.87	54.08	8.61	30.40	A	3.82	48.76	7.92	12	29.90
						B	3.06	43.87	6.96		
15		4.94	163.59	17.31	38.80	A	4.91	166.29	17.05	2	38.50
						B	4.94	167.06	17.39		
16		4.94	163.59	17.31	38.8	A	4.81	164.84	17.33	21	37.80
						B	6.24	209.86	22.02		

Tab.2

EXPERIMENTAL RESULTS

SECTION	TYPE	Fult kN	Mult kNm	ΔM %
1	A	0.78	0.20	10
	B	0.90	0.22	
2	A	2.41	0.61	37
	B	3.83	0.97	
3	A	3.95	1.01	13
	B	4.55	1.18	
4	A	4.67	1.19	5
	B	4.91	1.25	
5	A	4.19	1.06	0
	B	4.19	1.06	
6	A	4.97	1.25	1
	B	4.91	1.25	
7	A	3.59	0.91	9
	B	3.29	0.83	
8	A	4.31	1.09	4
	B	4.13	1.04	
9	A	4.73	1.19	5
	B	4.43	1.13	
10	A	2.39	0.61	53
	B	5.15	1.30	
11	A	8.62	2.16	12
	B	7.54	1.90	
12	A	8.10	2.03	16
	B	9.55	2.41	
13	A	11.81	2.96	13
	B	10.12	2.55	
14	A	10.74	2.70	10
	B	9.64	2.42	
15	A	18.63	4.61	11
	B	16.35	4.11	
16	A	19.85	4.74	28
	B	24.02	6.54	

Tab.3

2.3 Interpretation of experimental data

In term of ultimate behaviour, all specimens have shown similar collapse mechanism independently of the value of maximum load F_{ult} . Failure is always characterized by sudden crippling at one top corner. This phenomenon usually occurs in a cross-section located in the central part of the specimen, where the bending moment is constant. Regarding the ultimate load, the experimental results evidence in most cases a significant difference between the values obtained for the two tests on the same specimen (type A and B). Such a difference, given in tab.3 as percent scatter between the values of ultimate bending moments, ranges from a minimum of 0% obtained for the profile n.5 to a maximum of 37%, excluding the specimen n.10 which gave anomalous results also from the tensile tests. If the actual dimensions of specimens are accounted for, the analysis of test values of F_{ult} evidences that, except for the profile n.10, the scatter usually does not exceed 10% in terms of maximum stress.

The experimental response in term of force versus displacement relation-ship for all specimens belonging to the first group emphasized an elastic behaviour almost linear until the failure (fig.4), whereas for specimens of second group a premature decreasing in stiffness is observed due to the spread of local buckling phenomena (fig.5). This trend is amplified as far as the slenderness of the compression flange increases (profiles n. 3, 5, 7, 9).

The values of curvature (χ) for the examined cross-sections have been determined by means of strain measured at the top and bottom flanges. Therefore, the moment versus curvature behaviour is primarily influenced by the value of strain in the compression flange, since the tensile one virtually remains elastic. For specimens of first group these curves show an initial linear trend which later on becomes non linear due to yielding occurring in compression flange and local buckling at the web, the last phenomenon being more frequent in case of deepest shapes (fig.6). The second group of specimens provides a very irregular trend in the $M-\chi$ curves, being influenced by both local buckling of the top flange and yielding of the tensile one (fig.7). Local buckling usually affects the behaviour even for low values of loads and leads to very discontinuous curves. Yielding of the bottom flange affects the behaviour for large curvature values, sometimes leading to quasi-flat branches.

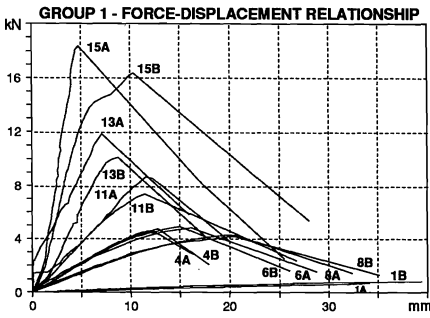


fig.4

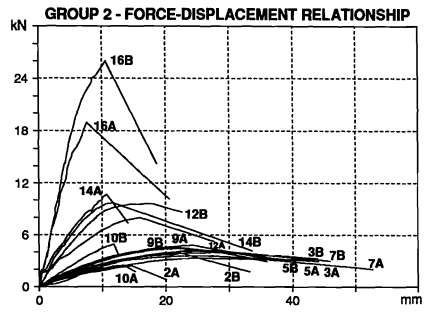


fig.5

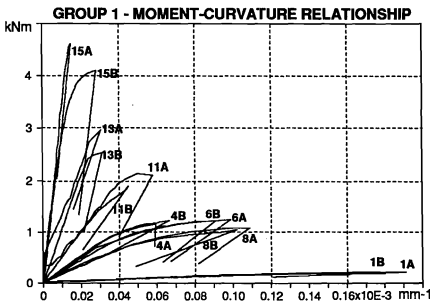


fig.6

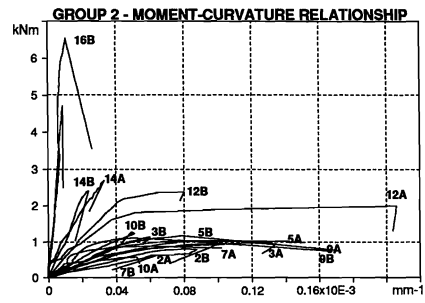


fig.7

3. THEORETICAL INVESTIGATION

3.1 Numerical simulation

The analysis of the bending process of investigated profiles has been numerically performed by means of a simulation method, which has been set up in the range of activity of a more general investigation on the bending behaviour of thin walled sections [7]. The cross-section is modelled by subdividing it in several small areas, where is possible to associate a residual strain, a local stress-strain relationship together with all informations needed for the knowledge of the load history. The deformation process of the section is examined with small consecutive increasing of curvature. For each curvature an iterative procedure gives the position of neutral axis, the strain and stress in each area (taking into account eventual local unloading) and the subsequent bending moment. Local buckling of compressed part is taken into account according to the theory of stability by using different interpretative models.

The practical use of the simulation procedure in the analysis of tested specimens, does not present particular difficulties in comparison with the application to cold-formed thin-walled sections as it has been done for other purpose [8]. It is mainly due to the simplicity of cross-section geometry, which is characterized by all flat element without intermediate stiffeners. With regard to buckling model, the elastic formulation in terms of strain has been adopted both in elastic and post-elastic field.

The simulation procedure has allowed to obtain the moment-curvature diagram for each specimen, by assuming the actual dimensions of cross sections and the material properties provided by above mentioned tension tests.

The comparison between the experimental $M-\chi$ curves and the simulation ones has shown, in many cases, a rather approximate agreement both in term of ultimate strength and stiffness. These differences are due to variability of material strength, according to scatter values found in tensile tests, as well as to initial geometrical imperfections. With regard to geometrical imperfections, they are taking into account by the proposed model only in post-buckling range. As a consequence the main differences have been found for specimens belonging to the first group, whose critical load is particularly high. On the contrary, for specimens of second group, the results provided by the simulation procedure have shown a better agreement with the experimental evidence, being the local buckling occurred even for low values of load.

In order to overcome these uncertainties a band criterium has been, therefore, assumed. According to this assumption the values of yielding stress ranged from the characteristic values ($f_{y,k}=271 \text{ Nmm}^{-2}$) to the experimental one ($f_{y,exp}$) have been considered. The lowering in stiffness due to initial geometrical imperfections, only for specimens belonging the first group, has been fortetarily evaluated by using an additional scatter band defined by two values of the elastic modulus: the nominal one ($E=206000 \text{ Nmm}^{-2}$) for the upper bound and a conventional reduced value ($E=175000 \text{ Nmm}^{-2}$) as lower bound in order to indirectly include the effect of geometrical imperfections. The comparison between the range of simulated curves and the experimental data, drawn in fig.8 and fig.9, for typical profile belonging to the first and second group respectively, shows that the band criteria allows a good interpretation of the experimental moment versus curvature results. The ratios between the ultimate moment given by the tests (M_{ult}) and by simulation corresponding to the upper (M_{s1}) and lower bound (M_{s2}) of the range criterium, are shown in fig.10 and fig.11.

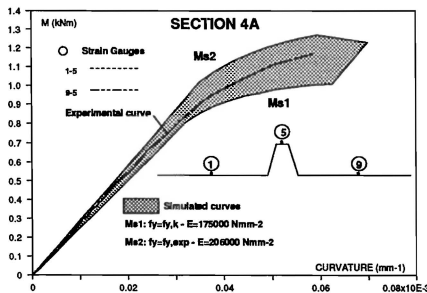


fig.8

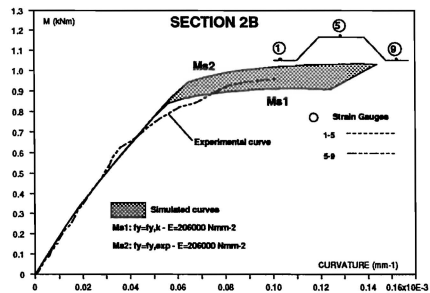


fig.9

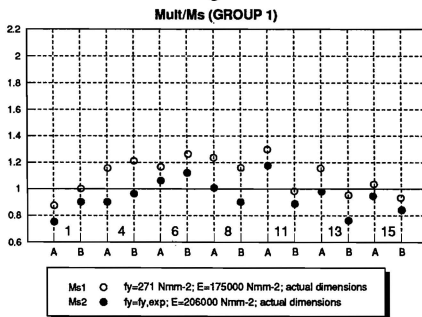


fig.10

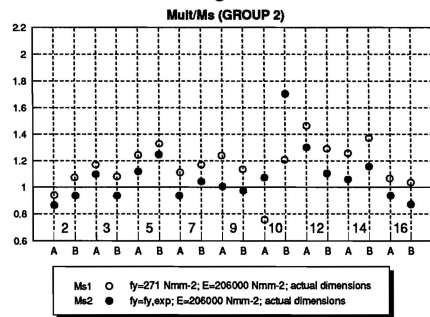


fig.11

3.2 Codes

The evaluation of design moments M_d on the basis of the criteria provided by Italian (CNR 10022 [9]), European (EC3-Part 1.3 [10]) and American (AISI [11]) codes has been performed. In order to have a unified parameter, which overrides the differences among the mentioned codes (allowable stress or ultimate limit state approaches), the design moment is defined as follow:

$$M_{d1} = W_{eff} \cdot f_{y,d} \quad (1)$$

being

W_{eff} effective section modulus evaluated according to each code, with reference to the nominal dimensions of specimens;

$f_{y,d}$ nominal yield stress for Fe E 250 G steel grade ($f_{y,d}=250 \text{ Nmm}^{-2}$)

This approach is usually followed in design procedure. As an alternative, the calculation of M_{d2} has been carried out by considering actual dimensions of the specimens and characteristic value of the yield stress ($f_{y,k}$).

The ratios between M_{ult} and the design moments provided by considered codes are shown in fig. 12 and 13 respectively for 1th and 2th group.

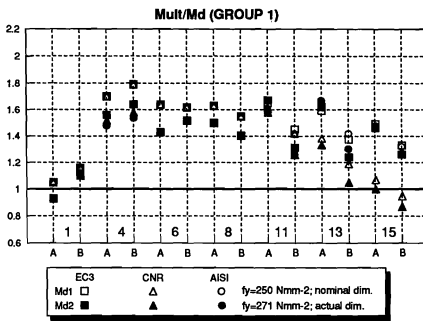


fig.12

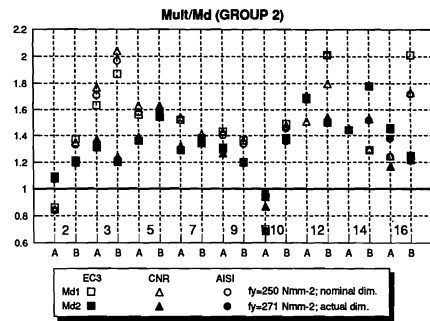


fig.13

4. ANALYSIS OF RESULTS AND COMPARISONS

The analysis of obtained theoretical results and the comparison with the experimental data allow to deduce some final remarks, which can be given separately for the two groups.

1th group: the numerical simulation gives a good correlation with the experimental results, since the scatters are always not larger than $\pm 25\%$, as shown in fig.10. When assuming $f_y=f_{y,exp}$, the numerical prediction (M_{s2}) leads to a better evaluation of the actual ultimate moments compared to that (M_{s1}) obtained when taking $f_y=f_{y,k}$. In particular for the profiles 8A, 13A and 4B the former assumption provides numerical values almost coincident with the experimental ones. The considered code provisions lead to very similar values of the design moments (fig.12), which in most cases are equal to the first yield moment of the geometrical cross-section ($M_d=M_y$), as it was expected. In fact, for profiles belonging to this group, local buckling phenomena are prevented since b/t is small. The most significant differences occur for the deepest profiles (nn.11, 13 and 15) whose failure is due to web buckling: in fact, such effect is accounted for by the codes with additional provisions. The design moments M_{d2} evaluated by introducing the

actual geometry and $f_y=f_{y,k}$ are in most cases closer to the experimental values compared to those (M_{d1}) computed by introducing the nominal values of geometrical dimensions and material properties.

2th group: even for this group, there is a good agreement between simulation and experimental results. The scatters are slightly large than those obtained for the first group; however the simulation usually provides a conservative estimate of the ultimate moments (fig.11). Once again the anomalous results provided by specimen n.10 are evidenced. The code provisions always give similar design moments which are smaller than M_y , due to the local buckling of the flange in compression (fig.13). The above observations can be justified by considering that the compared standards take into account flange local buckling in a similar way. As for the 1th group, the increase in the depth of specimens (profiles 12, 14 e 16) results in larger differences among the design moments provided by the codes, even if this tendency is less evident. Furthermore, the second approach (M_{d2}) gives a better agreement with test results.

Figures 14 and 15 report the mean values of the non-dimensional ratio between the test ultimate moments and the theoretical ones obtained by the numerical simulation and by the code provisions, in order to check the reliability of both approaches. It can be seen that the numerical model (fig.14) appears to be very suitable. In fact, for the 1th group, the simulation procedure provides, in the average, values of ultimate moments by 13% smaller than the actual ones, if $f_y=f_{y,k}$ is assumed, whereas it gives values of ultimate moment slightly larger (by 4%), if the actual strength of material is introduced. For profiles belonging to the second group, the simulation is always conservative, leading to scatter of 17% and 8% with respect to the experimental values.

The bearing capacity of sheets, evaluated according to the provisions of the Italian (CNR 10022), European (EC3-Part 1.3) and American (AISI) codes (fig.15), is underestimated by 50%, if nominal geometry of the cross-section and $f_{y,d}=250 \text{ Nmm}^{-2}$ are considered. The above scatter is reduced to 35%, if the actual geometry and $f_y=f_{y,k}$ are introduced. The previous observations can be extended to both groups of specimens, even if for the first one the variation in the mean scatters with the assumed code provisions increases.

5. CONCLUSIONS

The research programme described in this paper has been aimed at investigating the ultimate bending behaviour of standard trapezoidal sheets. In particular, experimental, theoretical as well as design aspects involved in this topic have been dealt with.

Tests have been performed on a large number of specimens, covering the most used shapes in practice.

The numerical simulation provides results in excellent agreement with the experimental ones, despite the large variation of shapes and the scatter in material properties.

The analysis of congruity of provisions given by the examined codes for cold-formed section has evidenced a large underestimation of the actual bearing capacity for this typologies of profiles. The mean value of the design moments, in fact, is usually smaller by 35-50% than the tests results.

Therefore, it can be concluded that the proposed numerical procedures can be used as an effective tool for carrying out a wide parametric analysis in order to develop more adequate design rules.

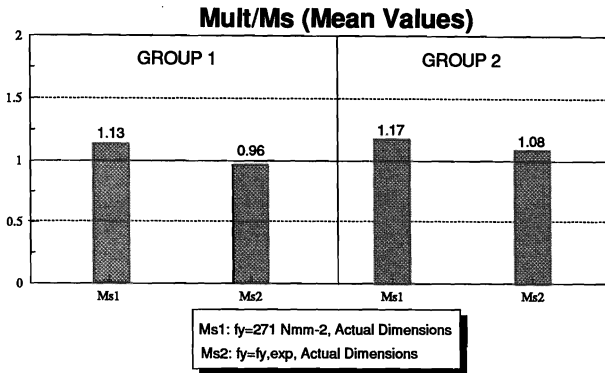


fig.14

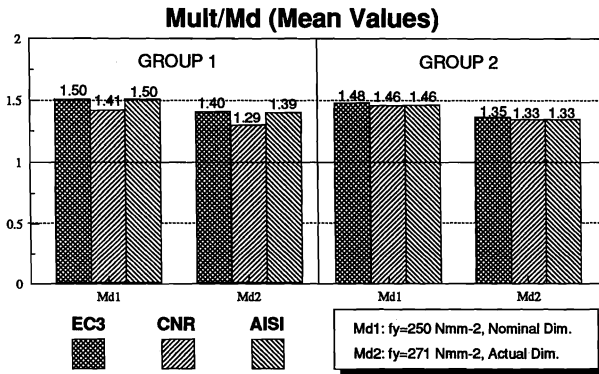


fig.15

ACKNOWLEDGEMENTS

This research has been coordinated by Prof. Dr. Ing. F.M. Mazzolani with the collaboration of Dr. Ing. R. Landolfo both from the Institute of Tecnica delle Costruzioni of the Engineering Faculty of the University of Naples. The research programme, sponsored by CREA (Dr. Morando), has been planned and agreed by Dr. Buzzichelli, Dr. Bufalini, Dr. Ing. Demofonti and Dr. Ing. Fattorini of CSM (Centro Sviluppo Materiali) in Rome. Tests have been performed at CSM laboratory by Dr. O. Vittori and E. Panzanelli. The specimens have been generously provided by Tubi Sud Italia (TSI) in Avellino.

APPENDIX - REFERENCES

1. Landolfo R., Mazzolani F.M., Behaviour of 3rd generation trapezoidal steel sheetings, Testing of Metals for Structures, RILEM Proceedings 12, E & FN SPON, Naples, May 1990.

2. De Martino A., Ghersi A., Landolfo R., Mazzolani F.M., Bending behaviour of long-span steel sheeting: test and simulation, Proceedings of International Conference on Steel e Aluminium Structures, Singapore, May 1991.
3. Bernard E.S., Bridge R.Q., Hancock G.J., Intermediate stiffeners in cold-formed profiled steel decks, Research Report No. R653-R658, University of Sydney, Australia 1992.
4. Panzanelli E., Vittori O., Studio teorico-sperimentale sul comportamento flessionale delle lamiere grecate per coperture, - Experimental activity - Research No.70521, Centro Sviluppo Materiali, Roma, October, 1992.
5. Landolfo R., Mazzolani F.M., Studio teorico-sperimentale sul comportamento flessionale delle lamiere grecate per coperture, Research Report No.70521, Centro Sviluppo Materiali, Roma, February 1993.
6. Landolfo R., Mazzolani F.M., Flexural tests on trapezoidal steel sheets, Proceedings of XIV Congress C.T.A., Viareggio, October 1993.
7. Mazzolani F.M., Thin-walled metal construction: research, design and codification, Proceedings of XIV Congress S.S.R.C., June 1994.
8. De Martino A., Ghersi A., Landolfo R., Mazzolani, F.M., Calibration of a bending model for cold-formed sections, Proceedings of 11th International Specialty Conference on Cold-Formed Steel Structures, University of Missouri-Rolla, Ottobre 1992.
9. CNR 10022:"Profilati di acciaio formati a freddo. Istruzioni per l'impiego nelle costruzioni", 1984.
10. Eurocode No.3 - Part 1.3 -, "Cold-formed Thin-gauge, Members and Sheeting", 1992.
11. A.I.S.I.:"Specification for the Design of Cold-Formed Steel Structural Members", American Iron and Steel Institute, 1986.

APPENDIX - NOTATION

a	total width of specimen
b	width of compressed flange
c	distance between tensile flange
h	height of section
t	sheet thickness
A	gross cross area
P	weight
I_x	second moment of area A
W_x	section modulus of gross cross area
W_{eff}	section modulus of effective cross area
E	Young modulus
f_y	yield stress of steel
$f_{y,d}$	nominal yield stress of steel
$f_{y,k}$	characteristic yield stress of steel
$f_{y,exp}$	experimental yield stress of steel
f_t	ultimate tensile strength of steel
$f_{t,d}$	nominal ultimate tensile strength of steel
$f_{t,k}$	characteristic ultimate tensile strength of steel
M	bending moment
M_y	yielding bending moment of gross cross section
M_d	design bending moment
M_s	simulated bending moment
M_{ult}	ultimate bending moment
F_{ult}	ultimate force
χ	curvature

